Article

Not peer-reviewed version

Numerical Assessment of the Thermal Performance of Microchannels with Slip and Viscous Dissipation Effects

Pamela Vocale * and Gian Luca Morini

Posted Date: 10 October 2024

doi: 10.20944/preprints202410.0834.v1

Keywords: slip flow; viscous heating; noncircular cross-sections; single gas flow

Article

Numerical Assessment of the Thermal Performance of Microchannels with Slip and Viscous Dissipation Effects

Pamela Vocale [1] and Gian Luca Morini [2,*]

[1] Department of Engineering and Architecture, University of Parma, Parma, Italy
[2] DIN – Alma Mater Studiorum Università di Bologna, Viale Risorgimento 3, 40135 Bologna, Italy; gianluca.morini3@unibo.it
* Correspondence: pamela.vocale@unipr.it

Abstract: In the present paper, a numerical analysis of the performance of microchannels featuring rectangular, trapezoidal, and double-trapezoidal cross-sections is presented. The fully developed laminar forced convection of a Newtonian fluid with constant properties is considered. The non-dimensional forms of governing equations are solved by setting slip velocity and uniform heat flux as boundary conditions. Model accuracy was established using the available scientific literature. The numerical results indicate that viscous dissipation effects led to a decrease in the average Nusselt number across all microchannels examined in this study. The degree of reduction is influenced by the cross-section, aspect ratio and Knudsen number. The lowest average Nusselt number values were observed under continuum flow conditions for all the microchannels investigated.

Keywords: slip flow; viscous heating; noncircular cross-sections; single gas flow

1. Introduction

The performance of microchannels, integral components in various microfluidic and heat transfer applications, is significantly influenced by factors such as rarefaction and viscous dissipation. As devices shrink to the microscale, the traditional assumptions of continuum fluid mechanics and inviscid flow often become invalid, necessitating a deeper analysis of these effects [1].

Rarefaction occurs when the mean free path of gas molecules approaches the same scale as the characteristic dimensions of the microchannel.

Viscous dissipation refers to the conversion of kinetic energy into thermal energy due to viscous forces within the fluid. In microchannels, this effect is pronounced due to the high surface-to-volume ratio, which leads to significant heating of the fluid. Viscous dissipation can alter the temperature profile, influence heat transfer rates, and impact the thermal management of microfluidic devices. This is particularly important in applications involving high flow rates or highly viscous fluids, where thermal effects can compromise the performance and reliability of the system [1].

The combined effects of rarefaction and viscous dissipation create a complex interplay that influences microchannel performance. Rarefaction can reduce frictional losses and modify flow characteristics, while viscous dissipation can lead to increased temperatures and affect fluid properties. Analyzing these effects requires an integrated approach that considers both fluid dynamics and thermal phenomena.

The effects of rarefaction and viscous heating on slip flows with uniform heat flux at the wall have been studied in microchannels featuring several cross-sections (i.e., circular, rectangular, elliptical, and rhombic cross-sections). In particular, the impact of viscous dissipation on circular microchannels was investigated by Tunc and Bayazitoglu [2], who considered only two Brinkman number values: Br = 0.01 and Br = – 0.01. Their findings showed that the Nusselt number can be

 doi:10.20944/preprints202410.0834.v1

reduced up to 8% for $Br = 0.01$. The investigation of the viscous dissipation influence on the convective heat transfer in microducts was extended by Aydın and Avcı [3] by considering more Brinkman numbers.

The effect of viscous dissipation on the Nusselt number in rectangular microchannels was studied by van Rij et al. [4]. Their results, presented only for two values of the Brinkman number (i.e., $Br = 0.05$ and $Br = -0.05$), highlighted that for Br = 0.05, the Nusselt number exhibited a maximum rate of change of approximately 24%.

The influence of viscous dissipation in elliptical microchannels was studied by Vocale et al. [5] by considering several values of the aspect ratio of the ellipse and several values of the Brinkman number. They found that the Nusselt number exhibited a maximum rate of change of approximately 30%.

Recently, the impact of viscous heating on rhombic microchannels was studied by Vocale et al. [6]. Their findings, presented for many values of the side angle and the Brinkman number, reveal that the Nusselt number exhibited a maximum rate of change of approximately 25%.

Viscous dissipation effects in trapezoidal microchannels characterized by an apex angle equal to 54.74° were analyzed by Kuddusi [7] by considering three sides of the cross-section heated, and one was considered adiabatic. Their findings, presented only for a value of the Brinkman number (i.e., $Br = 0.005$), reveal that the Nusselt number exhibited a maximum rate of change of approximately 2%. Moreover, they presented the rate of change in the Nusselt number for different values of the Brinkman number (i.e., up to 0.5), but only for an aspect ratio equal to 0.4.

Slip flows in double-trapezoidal (hexagonal) microchannels have been investigated by many researchers [8], who have also presented simplified slip models to evaluate the friction factors in polygonal microchannels. The thermal analysis of gaseous flows in double-trapezoidal (hexagonal) microchannels was performed by Sadasiva et al. [9], but by neglecting both rarefaction and viscous dissipation effects and by assuming H1 and T boundary conditions.

The literature review clearly indicates that understanding the effects of rarefaction and viscous dissipation is critical for the design and optimization of microfluidic systems.

Furthermore, the review highlights that existing data in the literature cover only a few values of aspect ratio, Knudsen number, and Brinkman number for rectangular microchannels. Finally, the literature review revealed that the analysis of slip flow in trapezoidal and double-trapezoidal (hexagonal) microchannels was investigated only in a few works, although these cross-sections are commonly used in various compact heat exchangers because they can be easily obtained by using chemical etching on silicon wafers.

In particular, trapezoidal microchannels are used in electronic cooling systems [10], while double-trapezoidal microducts are widely used in chemical applications [11].

To fill this gap, the present analysis offers a numerical analysis of the performance of rectangular, trapezoidal and double-trapezoidal microchannels. This study considered a Newtonian fluid with constant properties in fully developed laminar forced convection. The governing equations were solved using commercial software, with slip velocity and uniform heat flux along the wetted perimeter as boundary conditions. The model's accuracy was validated against the existing scientific literature.

The uniform wall heat flux boundary condition, identified as the H2 boundary condition in the literature (see Shah and London [12]), was selected because it is particularly useful in the presence of a microchannel with an imposed heat flux when solid walls are made with materials having a low thermal conductivity. In such cases, it is important to carefully monitor the rise in wall temperature along the wetted perimeter, especially near the corners of the cross-section, where temperature spots occur because of the stagnant fluid.

The insights gained from this study will contribute to the development of more efficient microchannels, improving the performance of various applications ranging from biomedical devices to cooling systems for electronic components.

2. Analysis

2.1. Mathematical Model

A gaseous flow in laminar fully developed forced convection in a microchannel with rectangular, trapezoidal, and double-trapezoidal cross-sections was considered (Figure 1). The investigated microchannels were characterized by an aspect ratio $\gamma = h/a$. Moreover, the trapezoidal microchannels presented an apex angle (α in Figure 1) equal to 54.74°, which is typically obtained by using chemical etching on silicon wafers as a manufacturing technology [5, 13]. A Cartesian system of coordinates x, y, and z is introduced with its origin in the cross-section center, as shown in Figure 1.

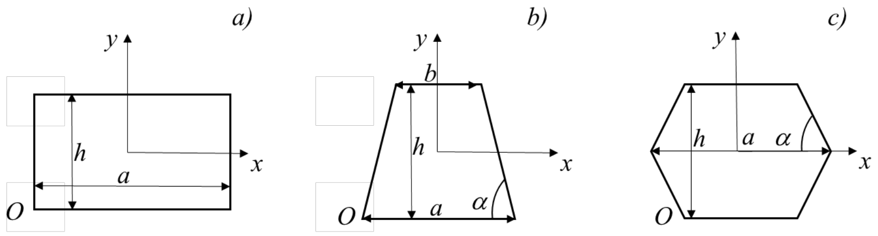

Figure 1. Microchannels under investigation: (**a**) rectangular; (**b**) trapezoidal; (**c**) double-trapezoidal.

The non-dimensional form of the Navier–Stokes equation can be written as follows:

$$\frac{\partial^2 u^*}{\partial^2 x^*} + \frac{\partial^2 u^*}{\partial^2 y^*} + p^* = 0 \quad (1)$$

where u^* and p^* indicate the dimensionless velocity and pressure gradients, respectively.

The non-dimensional form of the energy equation can be written as follows:

$$\frac{\partial^2 T^*}{\partial^2 x^*} + \frac{\partial^2 T^*}{\partial^2 y^*} = \frac{u^*}{A^*}\left(P^* + Br\int_{A^*} \Phi^* dA^*\right) - Br\Phi^* \quad (2)$$

where T^* is the dimensionless fluid temperature, A^* and P^* represent the dimensionless cross-section area and perimeter, respectively, (i.e., $A^*=A/D_h^2$ and $P^*=P/D_h$, being D_h the microchannel hydraulic diameter), Φ^* the viscous dissipation function in the non-dimensional form, and Br is the Brinkman number, which is defined as:

$$Br = \frac{\mu W^2}{q D_h} \quad (3)$$

In Equation (3), μ and W are the fluid dynamic viscosity and average velocity, respectively, and q is the wall heat flux imposed along the wetted perimeter. The first-order slip flow and temperature jump boundary conditions were applied to account for rarefaction effects [1]:

$$u^* - u_w^* = \frac{2-\sigma_v}{\sigma_v} Kn \left(\frac{\partial u^*}{\partial n^*}\right)_w \quad (4)$$

$$T_w^* = T^* + \frac{2-\sigma_T}{\sigma_T}\frac{2k}{k+1}\frac{Kn}{Pr} \quad (5)$$

where σ_v and σ_T are the momentum and thermal accommodation coefficients, respectively; Kn is the Knudsen number, which is defined as the ratio of the mean free path over the hydraulic diameter; k is the specific heat ratio; and Pr represents the Prandtl number.

It is interesting to observe how, under H2 boundary conditions, the wall temperature is only shifted of a constant value (which depends on the Knudsen number, the Prandtl number, the specific heat ratio and the thermal accommodation coefficient) with respect to the fluid temperature near the wall.

The average Nusselt number was calculated as follows:

$$Nu = \frac{hD_h}{\lambda} = \frac{1}{\overline{T_w^*} - T_b^*} \quad (6)$$

where h is the average convective heat transfer coefficient, λ the fluid thermal conductivity, $\overline{T_w^*}$ and T_b^* indicate the average wall temperature and fluid bulk temperature in nondimensional forms, respectively.

Equations (1-2) were solved by using equation-based modeling tools of COMSOL Multiphysics®. The solver relative tolerance was set to 1e–06. Quadratic shape functions have been used to solve both fluid velocity and temperature fields because of low flow velocities [14].

2.2. Mesh Independence Study

The mesh independence study was performed by considering three mesh refinements. For all generated meshes, the average Nusselt number was evaluated using Eq. (6). Nusselt number variations with the number of mesh elements for the microchannels investigated here are presented in Figures 2-4 for several Knudsen numbers. For the sake of brevity, the results of the mesh independence study are reported only for the smallest value of the aspect ratio considered here (i.e., γ = 0.1), which is the worst case (i.e., shallow microchannels) for testing numerical convergence. It can be observed that for a number of elements (*N*) higher than 500, Nusselt numbers are independent of mesh size for all the cross-sections analysed. The same findings were also observed for higher values of the aspect ratio.

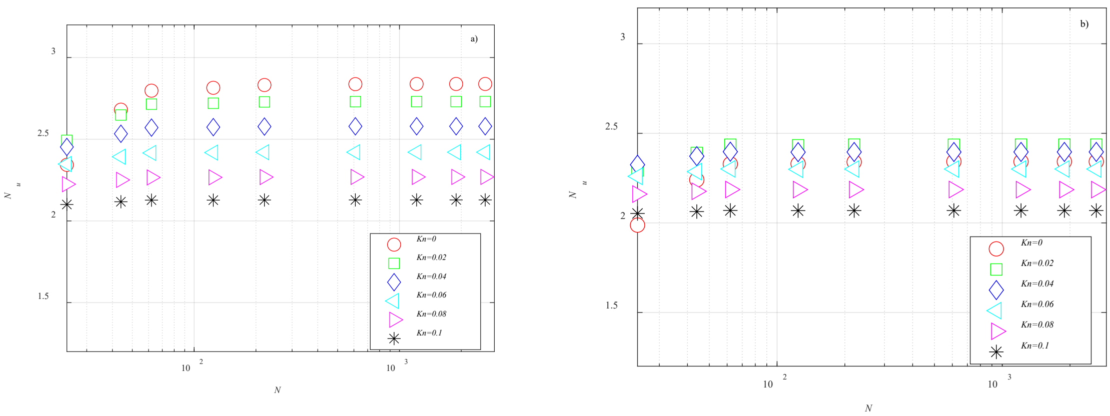

(**a**) (**b**)

Figure 2. Nusselt number variation with number of mesh elements for rectangular microchannel with γ= 0.1: (**a**) *Br* = 0.01; (**b**) *Br* = 0.1.

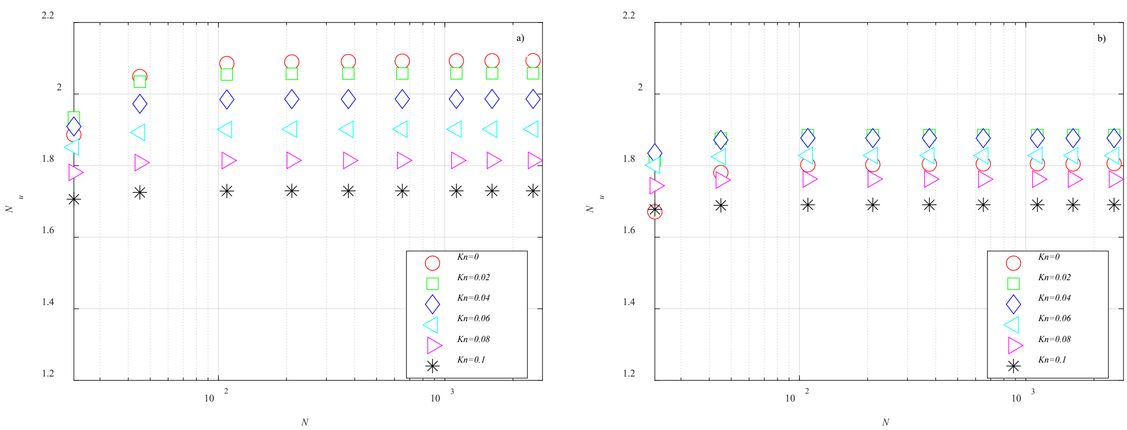

(**a**) (**b**)

Figure 3. Nusselt number variation with number of mesh elements for trapezoidal microchannel with γ = 0.1: (**a**) *Br* = 0.01; (**b**) *Br* = 0.1.

 doi:10.20944/preprints202410.0834.v1

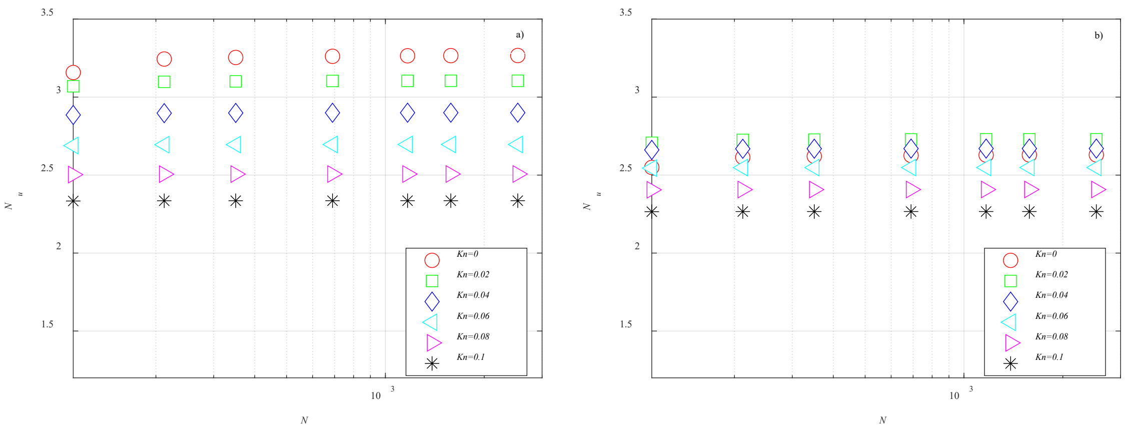

(**a**) (**b**)

Figure 4. Nusselt number variation with number of mesh elements for double-trapezoidal microchannel with $\gamma = 0.1$: (**a**) $Br = 0.01$; (**b**) $Br = 0.1$.

2.3. Model Accuracy

The model accuracy was established using the available scientific literature. In particular, because no experimental data are available in the literature, the numerical results obtained in the present analysis were compared only with numerical and analytical data. The numerical results for rectangular microchannels were compared with the results presented by van Rij et al. [4]. A perfect agreement was found, as shown in Table 1, where the comparison for $Br = 0.05$ was presented (i.e., the highest value of the Brinkman number considered in [4]).

Table 1. Comparison between Nusselt numbers for rectangular microchannels and the data presented in [4] for $Br = 0.05$.

γ	*Kn*	*Nu*	*Nu* [4]	Difference
0.2	0	2.600	2.585	-0.58%
	0.04	2.498	2.516	0.74%
	0.08	2.250	2.273	1.01%
0.5	0	2.617	2.616	-0.01%
	0.04	2.581	2.600	0.72%
	0.08	2.364	2.381	0.73%
1	0	2.651	2.647	-0.13%
	0.04	2.628	2.644	0.63%
	0.08	2.410	2.429	0.77%

The numerical results for trapezoidal microchannels were compared in Tables 2 and 3 with the data presented by Morini et al. [13] in terms of the Poiseuille number ($f\,Re$) within the slip flow regime and by Shah and London [12] in terms of the Nusselt in the continuum flow regime and without viscous dissipation. The agreement between the results reported in [12] and [13] and the present results validates the numerical procedure adopted in the present analysis.

Table 2. Comparison between the product $f\,Re$ for trapezoidal microchannels and the data presented in [13].

γ	*Kn*	$f\,Re$	$f\,Re$ [13]	Difference
0.047	0	22.298	22.174	0.56%
	0.1	10.425	10.355	0.67%
0.156	0	18.648	18.650	-0.01%
	0.1	9.274	9.269	0.05%

Preprints.org (www.preprints.org) | NOT PEER-REVIEWED | Posted: 10 October 2024 doi:10.20944/preprints202410.0834.v1

0.211	0	17.237	17.244	-0.04%
	0.1	8.823	8.829	-0.06%
0.293	0	15.566	15.565	0.00%
	0.1	8.288	8.281	0.09%
0.352	0	14.689	14.690	-0.01%
	0.1	8.008	8.006	0.02%
0.414	0	14.065	14.063	0.01%
	0.1	7.810	7.805	0.06%
0.452	0	13.830	13.832	-0.02%
	0.1	7.737	7.732	0.06%
0.522	0	13.657	13.654	0.02%
	0.1	7.677	7.674	0.04%
0.551	0	13.654	13.655	0.00%
	0.1	7.671	7.674	-0.04%
0.620	0	13.696	13.694	0.01%
	0.1	7.663	7.669	-0.07%
0.660	0	13.625	13.623	0.01%
	0.1	7.622	7.615	0.09%
0.707	0	13.311	13.308	0.02%
	0.1	7.485	7.479	0.07%

Table 3. Comparison between the Nusselt number for trapezoidal microchannels and data presented in [12] (i.e., for α= 60°, and $Br = Kn = 0$).

γ	***Nu***	***Nu* [12]**	**Difference**
0.109	2.337	2.310	1.16%
0.194	2.272	2.260	0.53%
0.317	2.216	2.200	0.74%
0.402	2.194	2.180	0.65%
0.465	2.184	2.170	0.64%
0.553	2.179	2.170	0.53%
0.604	2.180	2.170	0.41%
0.712	2.166	2.160	0.28%
0.782	2.094	2.090	0.18%

The numerical results for double-trapezoidal microchannels were also compared with the data presented by Morini et al. [13] and Shah and London [12]. Specifically, the results from [13] were expressed in terms of the Poiseuille number ($f\,Re$) in the slip flow regime, whereas the data from [12] were provided in terms of the Nusselt number in the continuum flow regime, excluding viscous dissipation. The agreement observed, as illustrated in Tables 4 and 5, can be considered satisfactory.

Table 4. Comparison between the product $f\,Re$ for double-trapezoidal microchannels and the results reported in [13].

γ	***Kn***	***f Re***	***f Re* [13]**	**Difference**
0.1	0	21.507	21.507	0.00%
	0.1	10.214	10.216	-0.02%
0.2	0	19.502	19.501	0.01%
	0.1	9.647	9.653	-0.06%
0.4	0	16.749	16.746	0.02%
	0.1	8.889	8.892	-0.03%
0.5	0	15.924	15.923	0.01%
	0.1	8.678	8.678	0.00%
0.6	0	15.405	15.403	0.01%

Preprints.org (www.preprints.org) | NOT PEER-REVIEWED | Posted: 10 October 2024 doi:10.20944/preprints202410.0834.v1

	0.1	8.551	8.549	0.03%
0.7	0	15.126	15.126	0.00%
	0.1	8.486	8.486	0.00%
0.8	0	15.028	15.027	0.00%
	0.1	8.463	8.460	0.04%
0.9	0	15.045	15.043	0.02%
	0.1	8.462	8.469	-0.08%
1.0	0	15.113	15.111	0.01%
	0.1	8.465	8.462	0.03%
1.2	0	15.083	15.081	0.01%
	0.1	8.386	8.385	0.01%
1.3	0	14.787	14.785	0.01%
	0.1	8.243	8.250	-0.09%
1.414	0	14.060	14.055	0.03%
	0.1	7.927	7.927	0.00%

Table 3. Comparison between the Nusselt number for double-trapezoidal microchannels and data presented in [12] (i.e., for α= 60°, and Br = Kn = 0).

γ	*Nu*	*Nu* [12]	Difference
0.866	3.8583	3.8620	-0.10%

3. Results and Discussion

The numerical results presented in this section cover different degrees of rarefaction by varying the Knudsen number and different aspect ratios. Specifically, the Knudsen number ranged from 0 to 0.1, while the aspect ratio γ varied from 0.1 to 1 for rectangular microchannels, from 0.1 to 0.707 for trapezoidal microchannels, and from 0.1 to 1.414 for double-trapezoidal microchannels. For a silicon microchannel, the aspect ratio is limited to a maximum value of tg(φ)/2, which is approximately 0.707 when φ = 54.74°. Beyond this point, the channel's cross-section degenerates into a triangular shape. The double-trapezoidal (or hexagonal) cross-sections considered in the present study were obtained from two trapezoidal microchannels, limiting the aspect ratio to a maximum value of 1.414 when φ = 54.74°. Beyond this threshold, the channel's cross-section transforms into a rhombic shape.

Additionally, nitrogen was assumed to be the working gas (i.e., Pr = 0.7 and k = 1.4), with both the momentum and thermal accommodation coefficients set to 1 [1].

3.1. Effect of Viscous Dissipation on Wall Temperature

Because viscous dissipation raises the fluid temperature at the wall, it is crucial to assess variations in wall temperature. From a practical standpoint, monitoring wall temperature is essential, particularly in applications where preventing it from reaching critical levels is mandatory.

The variation of the dimensionless wall temperature for rectangular microchannels with γ = 0.1, which represents the worst case (i.e., shallow microchannels) for fluid flow and heat transfer performances, is presented in Figure 4 for two values of the Brinkman number.

It can be observed that the non-dimensional fluid temperature varies significantly along the perimeter of the microchannel. This trend can be explained by recalling that the current analysis was conducted using a uniform wall heat flux boundary condition [12].

Moreover, it is evident that the wall temperature increased with an increasing Brinkman number. This effect can be explained by observing that viscous dissipation (Br) and rarefaction (Kn) play an opposite role: an increase in the wall slip velocity leads to a decrease in the velocity gradient, as well to a lower heat generation close to the walls due to viscous dissipation In Figures 4–6 the abscissa (s) corresponds to the length of the perimeter accounted for by starting from the point O in Figure 1.

Preprints.org (www.preprints.org) | NOT PEER-REVIEWED | Posted: 10 October 2024 doi:10.20944/preprints202410.0834.v1

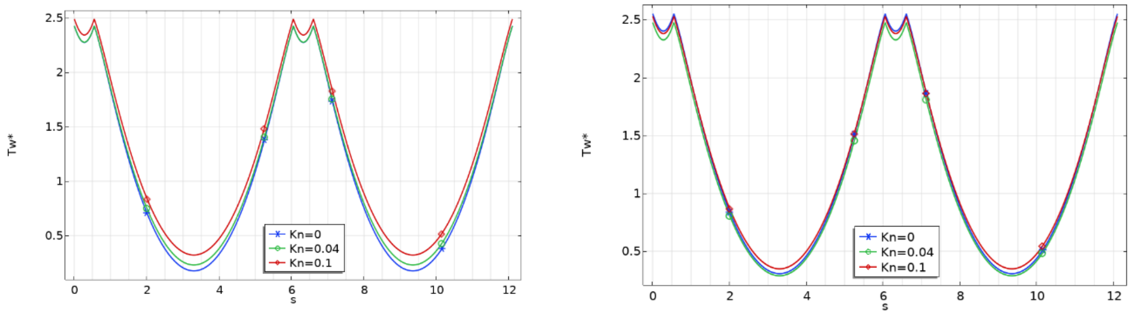

(**a**) (**b**)

Figure 4. Variation of the dimensionless wall temperature for rectangular microchannels with $\gamma = 0.1$: (**a**) $Br = 0$; (**b**) $Br = 0.1$.

The same findings are also obtained for trapezoidal and double-trapezoidal or hexagonal) microchannels, as shown in Figures 5 and 6, where the variation of the dimensionless wall temperature for $\gamma = 0.1$ is presented.

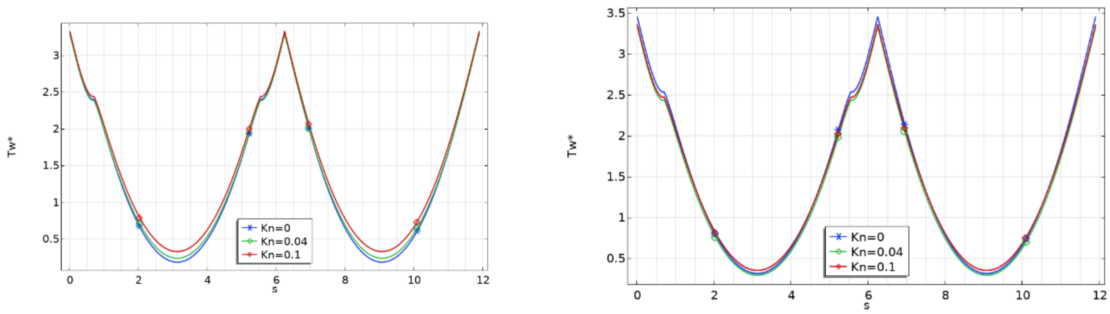

(**a**) (**b**)

Figure 5. Variation of the dimensionless wall temperature for trapezoidal microchannels with $\gamma = 0.1$: (**a**) $Br = 0$; (**b**) $Br = 0.1$.

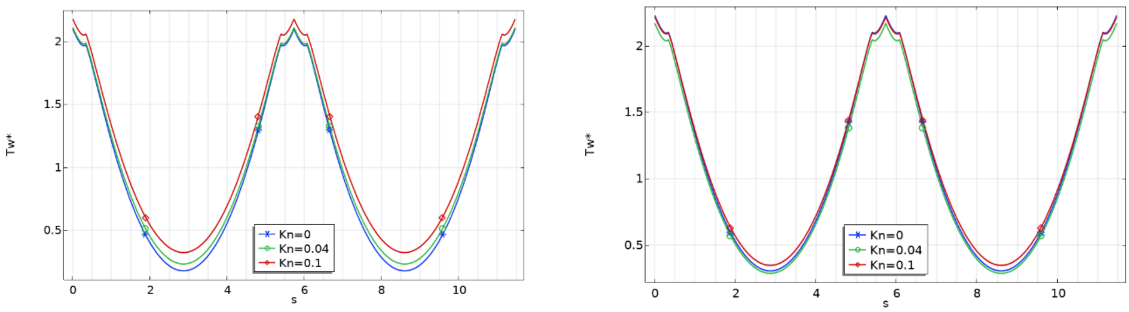

(**a**) (**b**)

Figure 6. Variation of the dimensionless wall temperature for double- trapezoidal (or hexagonal) microchannels with $\gamma = 0.1$: (**a**) $Br = 0$; (**b**) $Br = 0.1$.

3.2. Effect of Viscous Dissipation on the Nusselt Number

The thermal performance of the rectangular microchannels, in terms of the Nusselt number, is presented in Figure 7 for several Knudsen number values and two Brinkman number values. The data in Figure 7 show that for all values of the aspect ratio and the Knudsen number examined in this study, the Nusselt number decreases as the Brinkman number increases. This is because viscous dissipation generates thermal energy primarily near the wall, raising the fluid temperature at the

Preprints.org (www.preprints.org) | NOT PEER-REVIEWED | Posted: 10 October 2024 doi:10.20944/preprints202410.0834.v1

wall. This increases the temperature difference between the fluid bulk temperature and the average wall temperature, leading to a reduction in *Nu* (see Eq. (6)).

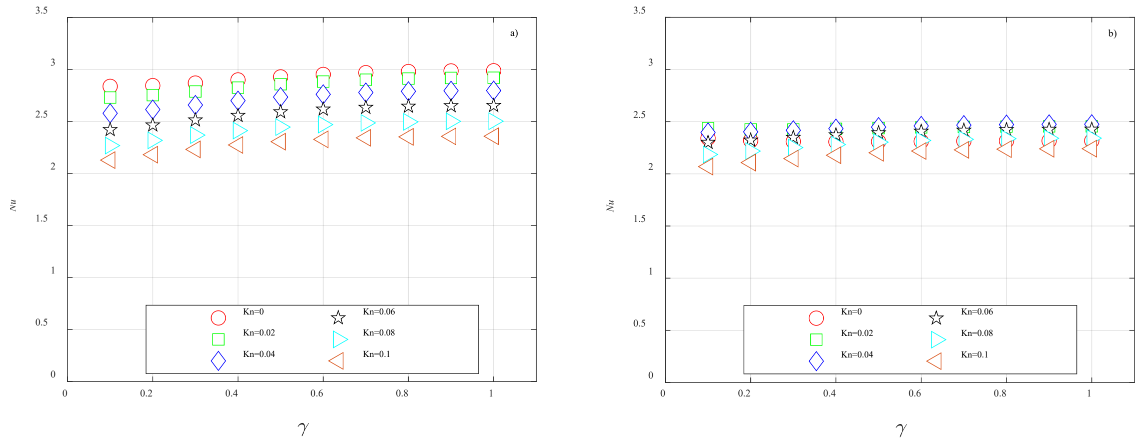

(**a**) (**b**)

Figure 7. *Nu* as a function of the aspect ratio in rectangular microchannels for different values of the Knudsen numbers: (**a**) $Br = 0.01$; (**b**) $Br = 0.1$.

The data in Figure 7 also reveal that the impact of viscous dissipation diminishes as *Kn* increases. For $\gamma = 1$ and $Kn = 0$, a *Br* of 0.1 results in a 25% decrease in *Nu*, whereas at $Kn = 0.1$, the same *Br* leads to only a 5.5% reduction in Nu. This reduced effect of *Br* on *Nu* at higher *Kn* values is attributed to lower velocity gradients due to the increased wall slip. The same findings were obtained by van Rij [4], who analysed only a few values of the aspect ratio and Brinkman number.

Figure 8 presents the thermal performance of the trapezoidal microchannels in terms of the Nusselt number for several values of the Knudsen and Brinkman numbers. The data shown in Figure 8 reveal that the well-known reducing impact of rarefaction on the Nusselt number is also confirmed for trapezoidal microchannels. Similar to the trend observed in [4] for trapezoidal microchannels characterized by different values of the apex angle, the Nusselt number decreased with an increasing aspect ratio. The influence of viscous dissipation is reduced for high Brinkman number values, even for trapezoidal cross-sections.

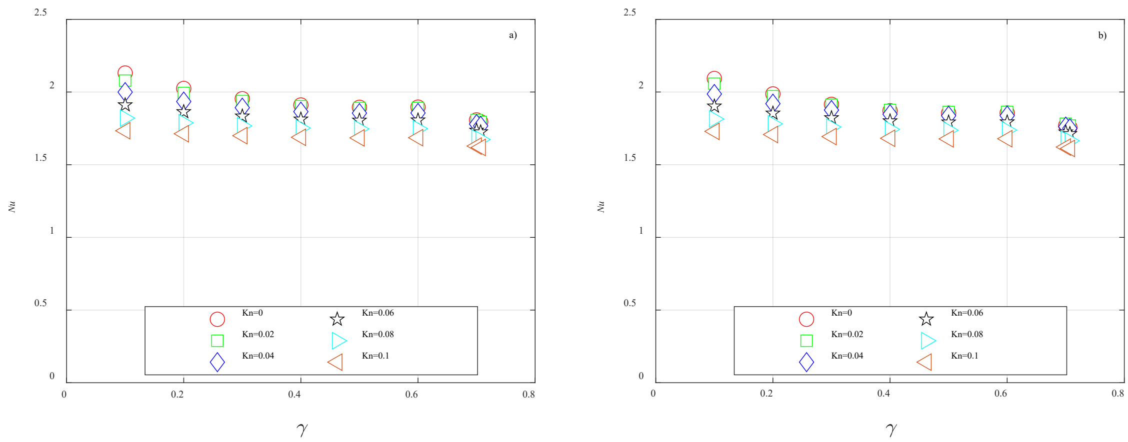

(**a**) (**b**)

Preprints.org (www.preprints.org) | NOT PEER-REVIEWED | Posted: 10 October 2024 doi:10.20944/preprints202410.0834.v1

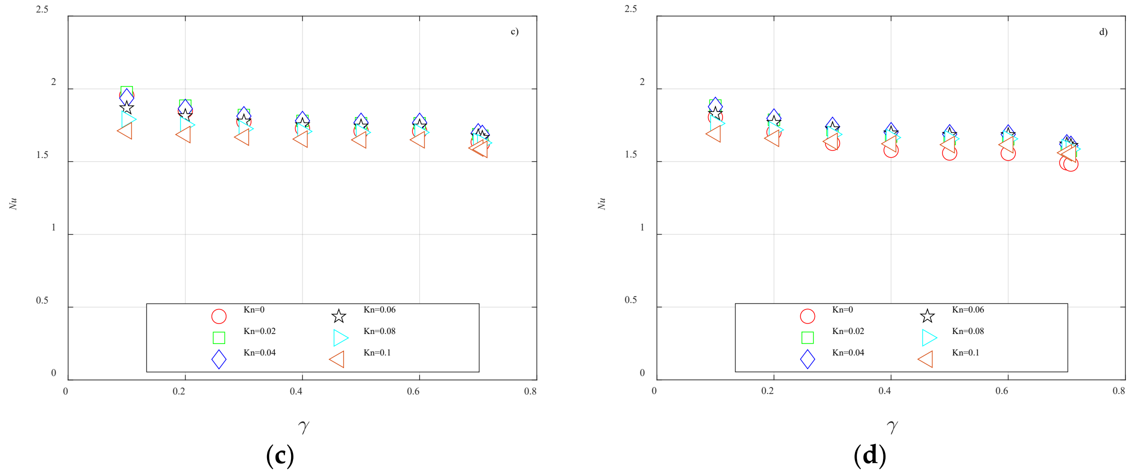

Figure 8. *Nu* as a function of the aspect ratio in trapezoidal microchannels for different values of the Knudsen numbers: (**a**) *Br* = 0; (**b**) *Br* = 0.01; (**c**) *Br* = 0.05; (**d**) *Br* = 0.1.

Figure 9 shows the variation of the Nusselt number with rarefaction and aspect ratio for double-trapezoidal (or hexagonal) microchannels. The data presented in Figure 9 reveal that the Nusselt number decreases as the Knudsen number increases for the double-trapezoidal (or hexagonal) microchannel. The one-way influence of the Knudsen number on the Nusselt number does not hold for the aspect ratio. The Nusselt number increases with the aspect ratio when $\gamma < 0.8$, reaches a maximum around $\gamma = 0.8$ and then decreases as the aspect ratio increases for $\gamma > 0.8$ for all values of the Brinkman number analysed in the present analysis.

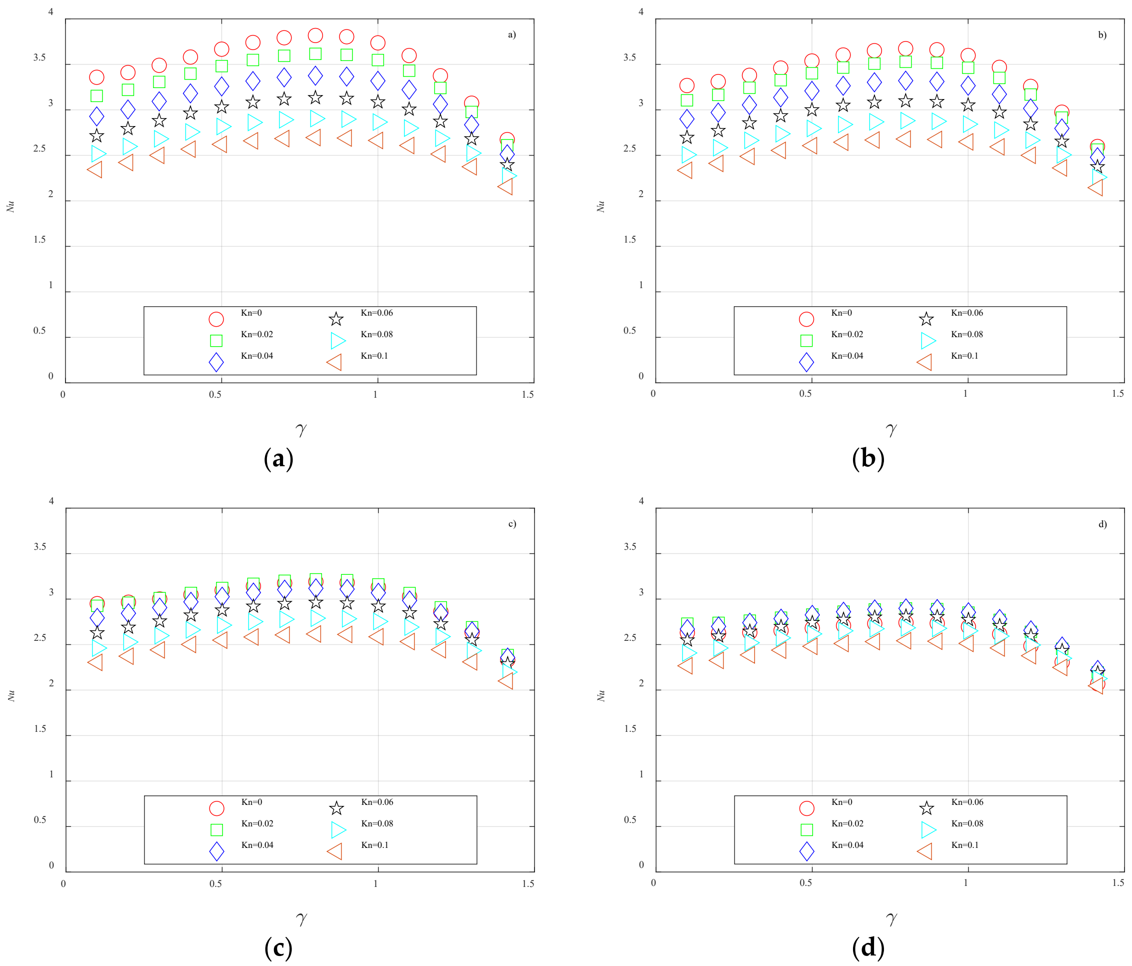

Figure 9. *Nu* as a function of the aspect ratio in double-trapezoidal (or hexagonal) microchannels for different values of the Knudsen numbers: (**a**) $Br = 0$; (**b**) $Br = 0.01$; (**c**) $Br = 0.05$; (**d**) $Br = 0.1$.

Similar trends were observed by Kuddusi et al. [7], who analysed the impact of the aspect ratio in trapezoidal microchannels by considering three sides of the cross-section heated, and one was considered adiabatic. They concluded that the observed trends in the Nusselt number were due to the considered thermal boundary condition.

4. Conclusions

This study presents a numerical analysis of the performance of microchannels with rectangular, trapezoidal and double-trapezoidal (or hexagonal) cross-sections. The numerical model used is comparable to those employed by various authors in the open literature for analyzing the slip-flow regime's effects on pressure drop and convective heat transfer coefficients.

The key conclusions drawn from the analysis are as follows:

- Viscous dissipation effects result in a decrease in the average Nusselt number for all the microchannels investigated here; the extent of reduction depends on the cross-section, the aspect ratio, and the Knudsen number.
- The lowest values of the average Nusselt number occurred under continuum flow conditions for all the microchannels investigated here.
- The Nusselt number exhibits a maximum rate of change of approximately 25% for rectangular microchannels.
- The Nusselt number exhibits a maximum rate of change of approximately 18% for trapezoidal microchannels.
- The Nusselt number exhibits a maximum rate of change of approximately 28% for double-trapezoidal (or hexagonal) microchannels.

The results presented here enable microthermal device designers to account for the effects of non-uniform wall temperature distribution in microchannels made with materials having poor thermal conductivity. In these cases, the imposed heat flux at the walls may cause thermal deformations in the channel walls due to the temperature spots close to the corners where the fluid is stagnant, especially for shallow microchannels. From this perspective, the numerical analysis provided here represents a valuable resource for designers and engineers involved in the sizing of compact heat exchangers, as well as Knudsen pumps.

Author Contributions: Writing—review & editing, P.V.; Supervision, G.L.M. All authors have read and agreed to the published version of the manuscript.

Funding: This research was funded by ITALIAN MINISTRY OF UNIVERSITY AND RESEARCH, National Recovery and Resilience Plan (NRRP), Mission 4 Component 2 Investment 1.5 - Call for tender No. 3277 of 30/12/2021 of Italian Ministry of University and Research funded by the European Union – NextGenerationEU. Award Number: Project code ECS00000033, Concession Decree No. 1052 of 23/06/2022 adopted by the Italian Ministry of University and Research, CUP D93C22000460001, "Ecosystem for Sustainable Transition in Emilia-Romagna" (Ecosister).

Data Availability Statement: The raw data supporting the conclusions of this article will be made available by the authors on request.

Conflicts of Interest: The authors declare no conflicts of interest.

References

1. Karniadakis, G.; Beskok, A.; Aluru, N. *Microflows and Nanoflows - Fundamentals and Simulation;* Springer: New York, 2005.
2. Tunc, G.; Bayazitoglu, Y.; Tunc, G.; Bayazitoglu, Y. Heat transfer in microtubes with viscous dissipation. *Int. J. Heat Mass Tran.* **2001**, *44*, 2395

 doi:10.20944/preprints202410.0834.v1

3. Aydın, O; Avcı, M. Heat and fluid flow characteristics of gases in micropipes. *Int. J. Heat Mass Tran.* **2006**, *49*, 1723–1730
4. van Rij, J; Ameel, T. Harman, T. The effect of viscous dissipation and rarefaction on rectangular microchannel convective heat transfer. *Int. J. Therm. Sci.* **2009**, *48*, 271–281.
5. Vocale, P; Puccetti, G.; Morini, G.L.; Spiga, M. Numerical Investigation of Viscous Dissipation in Elliptic Microducts. *J. Phys. Conf. Ser.* **2014**, *547*, 012023.
6. Vocale, P.; G Morini, G.L. Viscous dissipation effects on slip flow heat transfer in rhombic microchannels. *Int. J. Thermofluids* **2024**, *22*, 100619.
7. Kuddusi. L. First and second law analysis of fully developed gaseous slip flow in trapezoidal silicon microchannels considering viscous dissipation effect. *Int. J. Heat Mass Tran.* **2011**, *54*, 52–64.
8. Sadasivam, R.; Manglik, R.M.; Jog, M.A. Fully developed forced convection through trapezoidal and hexagonal ducts. *Int. J. Heat Mass Tran.* **1999**, 42 4321-4331.
9. Yovanovich, M.M.; Khan, W.A. Friction and Heat Transfer in Liquid and Gas Flows in Micro- and Nanochannels. In *Advances in Heat Transfer;* 1st ed.; Sparrow, E., Abraham, J., Gorman, J.; Elsevier Ltd.: Amsterdam, Netherlands, 2015, Volume 47, pp. 203–307.
10. Shah, R.K.; Sekulic, D.P. *Fundamentals of Heat Exchanger Design*. John Wiley & Sons, Inc., Hoboken, New Jersey, 2003.
11. Flockhart, S.M.; Dhariwal, R.S. Experimental and numerical investigation into the flow characteristics of channels etched in silicon. *J. Fluids Eng.* **1998**, *120*, 291–295.
12. Shah, R.K.; London, A.L. *Laminar flow forced convection in ducts*; Academic Press: New York, 1978.
13. Morini, G.L.; Spiga, M.; Tartarini, P. The rarefaction effect on the friction factor of gas flow in microchannels. *Superlattice Microst.* **2004**, *35*, 587–599.
14. COMSOL Multiphysics. 2023. Reference Manual.